Secondary reactions in electron-positron (electron) collisions*

Min-Shih Chen† and Peter Zerwas‡
Stanford Linear Accelerator Center, Stanford University, Stanford, California 94305
(Received 3 October 1974)

Secondary photon, electron, and positron beams are produced in colliding lepton-lepton rings. They induce inelastic electron Compton scattering and electron-photon scattering processes via photon-photon annihilation; likewise hard-photon bremsstrahlung belongs to this class of reactions. We study in detail the cross sections of these processes for high-energy lepton beams and discuss their physical significance.

I. INTRODUCTION

In conventional quantum electrodynamics, one lepton can interact with another lepton via exchange of virtual photons and/or leptons, as illustrated in Fig. 1. Hence, positron (electron)–electron colliding-beam machines might be viewed as a source of virtual photons, leptons, and antileptons which induce processes of the following types:

$$\text{photon}^* + \text{photon}^* \to \text{final state } f\ , \tag{1}$$

$$\text{photon}^* + \text{lepton} \to \text{final state } f\ , \tag{2}$$

$$\text{lepton}^* + \text{lepton} \to \text{final state } f\ . \tag{3}$$

The asterisks denote virtual particles; under specific kinematical conditions they can be very close to the mass shell, thus constituting equivalent secondary beams.[1]

However, there is a drawback in utilizing such secondary beams: The probability of emitting a secondary particle from the incident lepton is at most of the order of the fine-structure constant α, multiplied by the logarithm of the beam energy in units of the electron mass. In other words, the intensity of a secondary beam is suppressed by a factor $I \sim \alpha \ln(E/m_e)$ relative to the primary beam (I is of order 10^{-1} for presently operating machines). Therefore, experiments of the type (1)–(3) are feasible only if the cross sections are reasonably large and if the colliding-beam machines have sufficiently high luminosity. It is the purpose of this article to estimate the cross sections of certain processes of the types (1)–(3) and to study their physical significance.

For the moment, we put aside the question of whether there exist lepton-hadron interactions other than those expected from quantum electrodynamics. Then, two-photon processes of the type (1), such as

$$e^\pm + e^- \to e^\pm + \gamma^* + e^- + \gamma^*\ ,$$
$$\gamma^* + \gamma^* \to \text{hadrons}\ , \tag{1'}$$

illustrated by the first term on the right-hand side of Fig. 1(a), are physically most interesting. They have stimulated extensive theoretical discussions on specific properties of current-current couplings to hadrons.[2]

Another subject we shall study is processes of type (2), such as inelastic electron Compton scattering,

$$e^\pm + e^- \to e^\pm + \gamma^* + e^-\ ,$$
$$\gamma^* + e^- \to \text{hadrons} + e^-\ , \tag{2'}$$

illustrated by the second term on the right-hand side of Fig. 1(a). This process[3] is generally regarded as an annoying background to the more interesting two-photon process because the hadrons emerge from decaying virtual photons, but this coupling can be studied much more simply in direct e^+e^- annihilation. However, there is a kinematical configuration in which the process (2′) itself becomes interesting, namely, when the electron is scattered nearly backwards, as shown in Fig. 1(b). In this configuration, process (2′) dominates over the two-photon process, and the corresponding cross section attains a considerable size because the electron-propagator in the u channel of γe scattering can get very close to its pole. By varying the energy and angle of the final-state electron, the invariant mass M of the time-like virtual photon becomes a variable and can reach a value far below the total energy $2E$ of the incident $e^\pm e^-$ system. Therefore, this process allows us, in principle, to explore the photon propagator, or e^+e^- annihilation cross section, for very low values of M even with high-energy colliding-beam machines. Thus e^+e^- annihilation can be studied from the two-pion threshold up to the lowest energy directly available from e^+e^- beams. Even though the cross section for process (2′) is smaller by two orders of magnitude than direct low-energy electron-positron annihilation, it might be a valuable method if the luminosity of

high-energy rings is orders of magnitude larger than that of low-energy machines.

The Compton process has as a competitor the bremsstrahlung process[4,5]

$$e^+ + e^- \to \gamma + e^{+*} + e^- ,$$
$$e^{+*} + e^- \to \text{hadrons} . \qquad (3')$$

This is a reaction of type (3), and it is illustrated by the first term on the right-hand side of Fig. 1(c). By emitting a hard photon first, the subsequent e^+e^- annihilation can also take place at M^2 values much less than $4E^2$. There exists another diagram [the last term on the right-hand side of Fig. 1(c)] where the photon is emitted after the e^+e^- annihilation, leaving the final-state hadrons in a state of even charge conjugation. Certain aspects of this channel have been discussed in the literature.[4,6] Theoretically, both processes (2′) and (3′) are closely related to each other by crossing. Experimentally, the Compton process (2′) requires the detection of an electron very close to the direction of the incident positron (supposed to be the source of the almost real photon), while the annihilation process (3′) requires the detection of an energetic photon close to the beam direction. In both reactions, the final-state hadronic systems are produced with a sizable net momentum in the direction opposite to the detected e^- or γ. In the following, we shall discuss these cross sections in detail. They are typically of the order of 10^{-34} to 10^{-35} cm^2. As a general rule we find that low machine energy and fairly large M^2 favor the bremsstrahlung process (3′), while high machine energy and fairly low M^2 favor the Compton process (2′).

In the kinematical region where both leptons are scattered into their respective forward hemispheres (not necessarily with both scattering angles being small), the two-photon process[7] is more important than the Compton process; however, the latter can become an appreciable part of the background.[8] In the physically interesting case where the total invariant mass of the hadrons is large, this part of the background is determined by the large-M behavior of the photon propagator. With the recent data on high-energy e^+e^- annihilation,[9,10] this background becomes calculable, and it will be discussed in one of the following sections.

In Sec. II we formulate the cross sections for the Compton process (2′) and the bremsstrahlung process (3′), and we discuss some of their general properties. In Sec. III we consider both processes for specific final states in greater detail. In Sec. IV we calculate the contribution of the Compton process (2′) as a background to the two-photon process in $ee \to ee +$ hadrons; we discuss both the cross sections and the moments of the cross sections. Section V consists of some concluding remarks and a short discussion of related processes, such as electron-electron collisions in electron-positron machines.

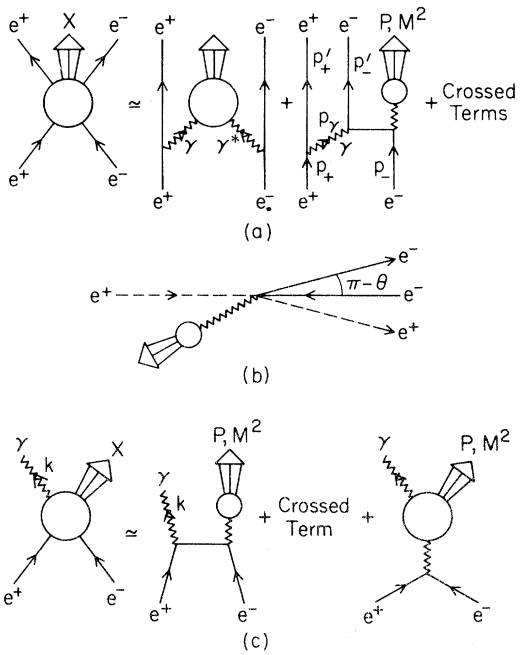

FIG. 1. (a) Production of a state $X(P, M^2)$ in electron-positron collisions via two-photon annihilation [$C(X) = +1$] and inelastic electron Compton scattering [$C(X) = -1$]; (b) kinematical configuration of particles if the Compton process is dominant; (c) hard-photon emission in e^+e^- annihilation via external bremsstrahlung off the lepton line [$C(X) = -1$] and out of the final system X [$C(X) = +1$].

II. GENERAL DISCUSSION

The cross section for inelastic electron Compton scattering,

$$e^- + \gamma \to e^- + \gamma^* \to e^- + f , \qquad (2'')$$

is straightforward to calculate if we average over the initial and sum over the final electron polarizations, and integrate over the momenta of the final state f. To the lowest order in α, the double differential cross section can be written as

$$\frac{d^2\sigma^{e\gamma \to ef}}{dM^2 dQ^2} \simeq \frac{\alpha}{2\pi} \frac{\sigma_f(M^2)}{s^2} \times \left[-\frac{u}{s} - \frac{s}{u - m_e^2} + \frac{2M^2Q^2}{s(u - m_e^2)} \right]. \qquad (4)$$

$\sigma_f(M^2)$ denotes the cross section for e^+e^- annihilation into the final state f. The electron rest mass

m_e is neglected in the numerators. The invariants s, t, u, M^2, and Q^2 are defined as

$$s=(p_\gamma+p_-)^2\ ,$$
$$t=(p_--p'_-)^2=(p_\gamma-P)^2\ ,$$
$$u=(p_\gamma-p'_-)^2=(p_--P)^2\ ,$$
$$Q^2=-t\ ,$$
$$M^2=P^2\ ,$$
$$s+t+u=M^2+2m_e{}^2\ ,$$

where p_γ, p_-, p'_-, and P are the four-momenta of the incident γ, the incident e^-, the scattered e^-, and the total final-state system f, respectively. In the center-of-mass (laboratory) system of the colliding beams we can write

$$p_\gamma=(E_\gamma,\,0,\,0,\,-E_\gamma)\ ,$$
$$p_-=(E,\,0,\,0,\,E)\ ,$$
$$p'_-=(E',\,0,\,E'\sin\theta,\,E'\cos\theta)\ ,$$

since the incident γ is predominantly collinear with the incident e^+, supposed to be the source of the Weizsäcker-Williams photon. If the scattered positron is not detected, we have to fold the cross section (4) into the photon spectrum. Using a simplified form for the equivalent photon spectrum in the laboratory frame[11]

$$N(E_\gamma)dE_\gamma=\frac{2\alpha}{\pi}\ln\frac{E}{m_e}\frac{dE_\gamma}{E_\gamma}\ , \tag{5}$$

the cross section for the Compton process in Fig. 1(a) is given by

$$\frac{d\sigma^{e\gamma}}{dM^2dQ^2}=\left(\frac{\alpha}{\pi}\right)^2\ln\frac{E}{m_e}\,\sigma_f(M^2)\times\int_{M^2}^{4E^2}\frac{ds}{s^3}\left[-\frac{u}{s}\frac{s}{u-m_e{}^2}+\frac{2M^2Q^2}{s(u-m_e{}^2)}\right]\ . \tag{6}$$

As shown in Fig. 2, the range of the kinematical variables Q^2 and $\nu=\frac{1}{2}(M^2+Q^2)$ is restricted to the interior of a triangle with the boundaries given by the lines $Q^2=0$, $Q^2=2\nu-M_0{}^2$, and $\theta=\pi$, where M_0 is the threshold energy for the final state f.

Leaving the details of the computation to the next section, we first estimate the cross section by integrating over the entire range of θ. In the most interesting case of $4E^2\gg M^2\gg m_e{}^2$, we obtain the approximate result

$$\frac{d\sigma^{e\gamma}}{dM^2}=2\left(\frac{\alpha}{\pi}\right)^2\frac{\sigma_f(M^2)}{M^2}\ln\frac{M}{m_e}\ln\frac{E}{m_e}\ , \tag{6'}$$

where the factor $\ln(E/m_e)$ comes from integrating the $(u-m_e{}^2)^{-1}$ pole term up to its maximum value at $u_{\max}\simeq -m_e{}^2M^2/(s-M^2)$. Two features of Eq.

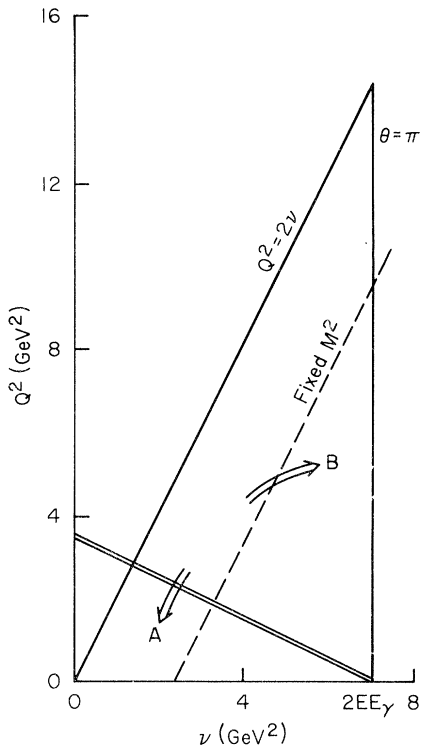

FIG. 2. (ν, Q^2) plane of electron-photon scattering for $E=3.5$ GeV and $E_\gamma=1$ GeV; the two-photon process dominates for small scattering angles of the electron (region A), the Compton process for large angles (region B); events with fixed electron scattering angle $\theta=30°$ fall onto the double line $Q^2=4E^2(1-\nu/2EE_\gamma)\tan^2(\frac{1}{2}\theta)$.

(6′) remind us of the equivalent photon approximation in two-photon processes[1]: (i) The factor α^2 is partially balanced by the logarithms of M and E in units of the extremely small electron mass; hence it is possible to obtain sizable cross sections even for such high-order electromagnetic processes. (ii) The factor M^{-2} strongly emphasizes the low-mass region of the final state f. Hence this process would be most suitable for studying threshold effects and low-M behavior of cross sections with high-energy colliding-beam machines. For both M and E in the range of a few GeV, we obtain as a rough estimate

$$\frac{d\sigma^{e\gamma}}{dM^2}\sim 6\times10^{-4}\,\frac{\sigma_f(M^2)}{M^2}\ . \tag{6''}$$

The analysis for specific final states $f=\mu^+\mu^-$, $f=\pi^+\pi^-$, and $f=$(all hadrons) and more detailed numerical results are discussed in the next section.

The final state f in the Compton process (2′) has odd charge conjugation C. This process competes with the two-photon process (1′), which produces final states of even C. Thus there is no inter-

ference between these two channels in the cross section if the phase space of the final-state particles is integrated over. Neglecting terms of higher order in α, the inclusive cross section for $e^{\pm}+e^{-}\to e^{\pm}+e^{-}+$anything is simply the sum of these two cross sections. The cross section for the two-photon process can be written as[7]

$$\frac{d\sigma^{\gamma\gamma *}}{dM^2dQ^2}=2\alpha^3\ln\frac{E}{m_e}\int\frac{dE_\gamma}{E_\gamma}\left[\frac{1}{\nu}\left(1-\frac{\nu}{2EE_\gamma}\right)F_2{}^{\gamma}(M^2,Q^2)+\frac{Q^2}{8(EE_\gamma)^2}F_1{}^{\gamma}(M^2,Q^2)\right]. \tag{7}$$

$F_{1,2}{}^{\gamma}(M^2,Q^2)$ are the structure functions of the real photon, defined in a way similar to the nucleon structure function in inelastic electron scattering. The cross sections (6) and (7) are dominant in two different phase-space regions, which can easily be seen from their pole structure. As a result of the pole at $t=-Q^2=0$, the cross section for the two-photon process is peaked near the forward direction $\theta\gtrsim 0$, whereas the $u=m_e{}^2$ pole in the Compton amplitude induces a backward peak.[8] Of course, for small θ, the Compton process is nothing but a radiative correction to the two-photon process. In Sec. IV we shall show that this correction is indeed small in two-photon experiments with the presently available machines.

In utilizing high-energy colliding-beam machines to explore the photon propagator (or equivalently the e^+e^- annihilation cross section) well below the machine energies, the Compton method competes with the well-known bremsstrahlung process (3′).[4,5] The reaction $e^+e^-\to\gamma f$ is simply related to the Compton process (2″) by $s\leftrightarrow t$ crossing. If

$$S=4E^2 \text{ and } T=(p_+-k)^2\ ,$$

where p_+ and k are the four-momenta of the incident positron and the radiated hard photon, respectively, the cross section for this process is given by

$$\frac{d\sigma^{\gamma}}{dT\,dM^2}=\frac{\alpha}{2\pi}\frac{\sigma_f(M^2)}{S}\left[\frac{U}{T-m_e{}^2}+\frac{T}{U}+\frac{2M^2S}{U(T-m_e{}^2)}\right], \tag{8}$$

where m_e is neglected in the numerators and U is given by

$$S+T+U=M^2+2m_e{}^2\ .$$

For $S\gg M^2\gg m_e{}^2$ and a photon energy of the order of E, we can easily integrate over all photon angles to obtain

$$\frac{d\sigma^{\gamma}}{dM^2}\simeq\frac{2\alpha}{\pi}\frac{\sigma_f(M^2)}{S}\ln\frac{E}{m_e}\ , \tag{8′}$$

keeping in mind that most of the contributions come from the small-T region where the photon is emitted along the direction of the incident positron. For E of a few GeV, we obtain the estimate

$$\frac{d\sigma^{\gamma}}{dM^2}\sim 4\times10^{-2}\frac{\sigma_f(M^2)}{S}\ . \tag{8″}$$

As easily seen from the above equation, the cross section decreases with the incident beam energy, but its M dependence is determined by $\sigma_f(M^2)$ alone. With $S\sim 10$ GeV^2 and $\langle\sigma_f\rangle\sim 50$ nb for $1\lesssim M^2\lesssim 10$ GeV^2, we obtain $d\sigma^{\gamma}/dM^2\sim 0.2$ nb/GeV^2. More detailed results will be presented in the next section.

The hard photon can also be radiated after the electron and positron have annihilated,[4,6]

$$e^+ + e^-\to\gamma^*\to\gamma+f'\ , \tag{9}$$

as illustrated by the last term on the right-hand side of Fig. 1(c). As a consequence of charge-conjugation invariance, there is again no interference between this background and the bremsstrahlung process when we integrate over the phase space of the final-state particles, the hard photon excepted. Without detailed information on the $\gamma^*\to\gamma f'$ vertex, it is difficult to calculate this background for any state f' other than pure leptonic ones, like $f'=\mu^+\mu^-$. However, we can argue on general grounds that (i) since there is no preferred direction for the hard-photon emission in process (9) while the photon is emitted in forward direction in the bremsstrahlung process, and (ii) since the cross section for the process (9) is suppressed relative to the bremsstrahlung process, such a background is expected to be small if hard photons are measured only near the forward direction.

Comparing the Compton method with the bremsstrahlung method, we can see that they are actually complementary to each other. The former is more suitable for studying the threshold behavior, namely, the low-M region of $\sigma_f(M^2)$ with high-energy beams, whereas the latter is more suitable for studying the transition region between the threshold and high-energy regions of $\sigma_f(M^2)$ with moderate-energy beams. A more specific comparison is carried out in the next section.

III. LOW-ENERGY e^+e^- ANNIHILATION

The low-energy behavior of the e^+e^- annihilation cross sections has not yet been experimentally explored. For example, the threshold behavior of the $\pi^+\pi^-$ production cross section, which is related to the pion form factor in the timelike region, has yet to be determined. A precise determination of the mean radius of the pion relies on this threshold behavior, as well as the hadronic contributions to the g factor of the electron. We devote this section to the study of the Compton and brems-

strahlung methods for such measurements, and we numerically estimate their cross sections. Of course, the cleanest experiment would be the direct measurement of e^+e^- annihilation, if possible.

To calculate the differential cross sections (with respect to M^2) for the Compton process, we numerically integrate Eq. (6) over the angle of the scattered e^- in the range $-0.99 \leq \cos\theta \leq 0$, which corresponds to $\pi - 0.04 \geq \theta \geq \frac{1}{2}\pi$. For the bremsstranlung process, we analytically integrate Eq. (8) over the angle of the emitted γ in the range $0.16 \leq \theta \leq \frac{1}{2}\pi$. Depending on the minimum angle that is experimentally accessible, the cross sections can be larger by a factor of about 2 than those obtained for the above range if θ is extremely close to the beam axis.

Let us first discuss the $\pi^+\pi^-$ production cross section. For this process, we have

$$\sigma_{f=\pi^+\pi^-}(M^2) = \frac{\pi\alpha^2}{3M^2}\left(1 - \frac{4m_\pi^2}{M^2}\right)^{3/2} |F_\pi(M^2)|^2 , \tag{10}$$

where m_π is the pion mass and $F_\pi(M^2)$ is the pion form factor. If the pions were pointlike, the cross section would be given by Eq. (10), with $F_\pi(M^2) \equiv 1$. In the range $0.6 \leq M \leq 0.8$ GeV, where $\sigma_{f=\pi^+\pi^-}(M^2)$ has been measured, the Gounaris-Sakurai formula[12] of the ρ-dominated pion form factor gives an excellent fit to the data.[13] To obtain an estimate for the cross section below 600 MeV, we thus use the Gounaris-Sakurai formula as well,

$$F_\pi(M^2) = \frac{m_\rho^2(1 + M^2/s_1)(1 + d_\rho\Gamma_\rho/m_\rho)}{m_\rho^2 - M^2 + m_\rho^2\Gamma_\rho[k^2(h - h_\rho) + (m_\rho^2 - M^2)k_\rho^2 h_\rho']k_\rho^{-3} + im_\rho^2\Gamma_\rho k^3/Mk_\rho^3} , \tag{11}$$

where

$$h(M^2) = \frac{2k}{\pi M}\ln\frac{2k+M}{2m_\pi} ,$$

$$k(M) = \tfrac{1}{2}(M^2 - 4m_\pi^2)^{1/2} ,$$

$$h_\rho = h(m_\rho^2), \quad k_\rho = k(m_\rho^2), \quad h_\rho' = (dh/dM)_{M=m_\rho} ,$$

$m_\rho = 0.774$ GeV is the ρ mass ,

$\Gamma_\rho = 0.111$ GeV is the ρ width ,

$s_1 = 9.6m_\rho^2 \times 10^6$, and $d_\rho = 0.48$.

Substituting Eqs. (11) and (10) into Eqs. (6) and (8) and integrating over θ, we obtain the $\pi^+\pi^-$ production cross sections for $0.35 \leq M \leq 0.65$ GeV. The results for the Compton process are shown in Figs. 3 and 4 and those for the bremsstrahlung process in Fig. 5. As a reference, we have also plotted the pointlike pion production cross sections for the Compton process in Fig. 3. Owing to the ρ enhancement, the cross section given by the Gounaris-Sakurai formula is larger than the pointlike cross section in this range.

As seen from Figs. 3 and 5, the Compton method is best for studying the pion form factor near threshold. The cross section is typically of the order of 10^{-34} cm^2/GeV^2. For a colliding-beam machine with a luminosity of 10^{31} to 10^{32} particles/sec cm^2, cross sections of such size should be measurable. The signature for these events is very clear. After emitting a nearly on-shell photon, the final-state positron moves nearly along the incident direction with a momentum comparable to E. However, the scattered electron accompanies the positron since the dominant contribution to the cross section stems from the u-channel diagram, which is related to the backward e^- scattering in the $e^-\gamma$ system. The pion pair is produced in the direction opposite to the final-state e^+e^- system. However, even though the total momentum of the pion pair is very close to the beam direction for $M \lesssim 3m_\pi$, each pion can have an opening angle of a few degrees in the laboratory frame. Radiative corrections will be discussed at the end of the

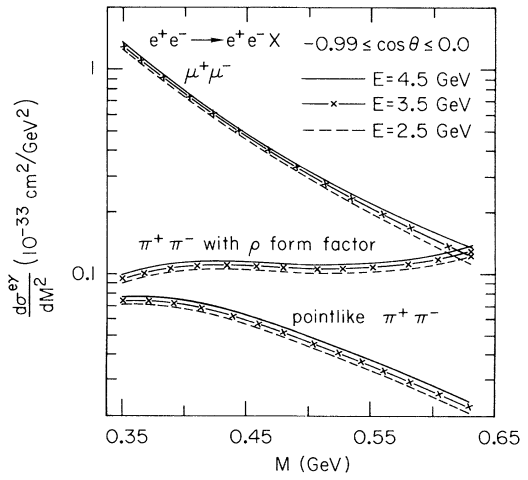

FIG. 3. Two-particle production in inelastic electron Compton scattering near threshold (M denotes the invariant mass of the two-particle system). The difference between the two $\pi^+\pi^-$ curves indicates the influence of the $\pi^+\pi^-$ form factor.

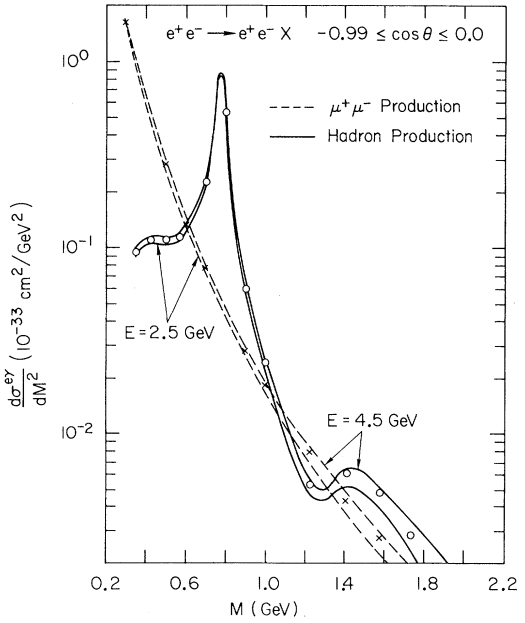

FIG. 4. Inclusive inelastic electron Compton scattering with M being the invariant mass of the decaying photon. Crosses and little circles indicate the size of the cross sections for beam energy $E=3.5$ GeV.

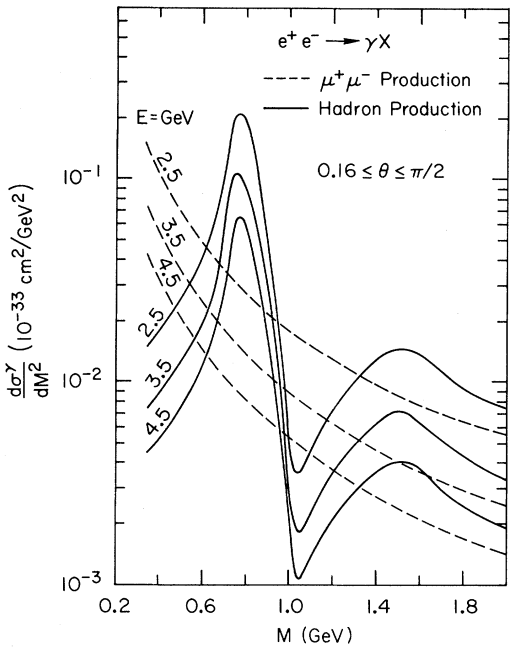

FIG. 5. Inclusive production of hadrons and $\mu^+\mu^-$ pairs in the hard-photon bremsstrahlung process.

section.

For M slightly higher than $2m_\pi$ it is very tempting to consider the three-pion production near threshold, since a measurement of this threshold behavior provides a test for the theory of chiral anomalies and the partial conservation of the axial-vector current (PCAC). The cross section has been estimated to be[14]

$$\sigma_{f=3\pi}(M)\simeq 3.7\times10^{-10}m_\pi^{-2}\left(\frac{M-3m_\pi}{m_\pi}\right)^4 . \qquad (12)$$

Substituting Eq. (12) into Eq. (6), the resulting cross section is of the order of 10^{-38} cm^2/GeV^2 for $3m_\pi \leq M \leq 4m_\pi$ and, therefore, too small to be experimentally accessible. Even in theories which predict a strong violation of PCAC[15] for $\gamma^* \to 3\pi$, the cross section is still only of the order of[16] 10^{-36} cm^2/GeV^2. The contribution to the three-pion production near threshold from the tail of the ρ meson is also as large as 10^{-38} cm^2/GeV^2. Therefore, it would be very surprising if one could see any three-pion production cross section at all near threshold.

For $M \geq 600$ MeV, various $\sigma_f(M^2)$ have been directly measured in e^+e^- annihilation. We estimate the cross sections in the region $600 \leq M \leq 1100$ MeV by the vector-meson-dominance model, namely,

$$\sigma_{f=\text{all hadrons}}(M^2)=\sigma_{f=\rho}(M^2)+\sigma_{f=\omega}(M^2)+\sigma_{f=\phi}(M^2) , \qquad (13)$$

where $\sigma_{f=\rho}(M^2)\simeq\sigma_{f=\pi^+\pi^-}(M^2)$. The ω and ϕ cross sections are

$$\sigma_{f=V}(M^2)=\frac{16\pi^2\alpha^2}{M^4}\,\frac{m_V{}^5\Gamma_V/f_V{}^2}{(m_V{}^2-M^2)^2+m_V{}^2\Gamma_V{}^2} , \qquad (14)$$

with[13] $V=\omega,\phi$: $M_\omega\simeq0.783$ GeV, $\Gamma_\omega\simeq0.012$ GeV, $f_\omega{}^2/4\pi\simeq13.4$, $M_\phi\simeq1.019$ GeV, $\Gamma_\phi\simeq0.004$ GeV, and $f_\phi{}^2/4\pi\simeq12.85$. For $M\geq1100$ MeV, including the ρ' region, we use the measured cross section[9,10] and a simple linear interpolation at values of M where no data are available. The resulting cross section for the Compton process is plotted in Fig. 4 and that for the bremsstrahlung process in Fig. 5. Notice that, due to the smallness of their widths, the ω and ϕ peaks are not resolved in these plots.

As discussed in Sec. II, the cross section for the Compton process increases whereas that for the bremsstrahlung process decreases with beam energy. In Fig. 6 we compare the M dependence of these two cross sections, with the former evaluated at $E=4.5$ GeV and the latter at $E=2.5$ GeV. We have already mentioned that the low-M region favors the Compton process. On the other hand, the sharp falloff in M makes the Compton process unsuitable for studying the e^+e^- annihilation cross section in the region $1\leq M^2\leq10$ GeV^2. Therefore, the bremsstrahlung process is a better candidate. This cross section is typically of the order of 10^{-35} cm^2/GeV and should be observable for a col-

liding-beam machine with a luminosity of 10^{32} particles/sec cm^2.

We shall conclude this section by discussing some questions concerning possible background reactions, radiative corrections, and the experimental normalization of the cross sections. As briefly discussed in Sec. II, there is a background, reaction (9), to the bremsstrahlung process. Both of these processes are of the same order in α. However, when the hard photon is emitted near the beam direction, the lepton propagator for the bremsstrahlung process is very close to the pole and the integrated cross section is enhanced by a factor of $\ln(E/m_e)$. On the other hand, the hard-photon emission in process (9) is not enhanced in any direction and, due to the difference in the masses of the timelike virtual photons, the cross section for the process (9) is suppressed by a factor M^2/S relative to the bremsstrahlung process. A simple quark-parton calculation[6] gives a cross section for the process (9) of the order of $\alpha\sigma_f(M^2)M^2/S^2$ which is indeed smaller by a factor of $(S/M^2)\ln(E/m_e)$ relative to Eq. (8′). If the hard photon is restricted to a small solid angle along either of the beam axes, we expect this part of the background to be negligibly small. For the Compton process in e^+e^- collisions, a similar background exists, namely

$$e^+ + e^- \to \gamma^* \to e^+ + e^- + f \ , \tag{15}$$

which is of the same order in α as the Compton and two-photon processes and is itself an interesting process. By arguments similar to those for (9), the contribution to the cross section from process (15) is also expected to be negligible if both of the final-state leptons are restricted to be inside a small solid angle along the incident positron beam direction.

Next we have to consider radiative corrections (mainly photon insertions on the lepton lines) in both the Compton and bremsstrahlung processes. Since these radiative corrections are of higher order in α and the final states are restricted to small angles, we expect the corrections to be small. Furthermore, radiative corrections mainly affect the absolute normalization of the cross sections, which is not important for the purpose of studying $\sigma_f(M^2)$. As can be seen from Eqs. (6) and (8), the ratio of $\sigma_f(M^2)$ for two different final states is equal to the ratio of the cross section for the Compton and/or bremsstrahlung processes and is independent of the absolute normalization of the cross sections. As a result, the normalization of $\sigma_f(M^2)$ can be fixed relative to some particular final state for which the e^+e^- annihilation cross section can be well determined. Such a candidate is $\mu^+\mu^-$ pair production, which is a purely leptonic reaction. From quantum electrodynamics, we have

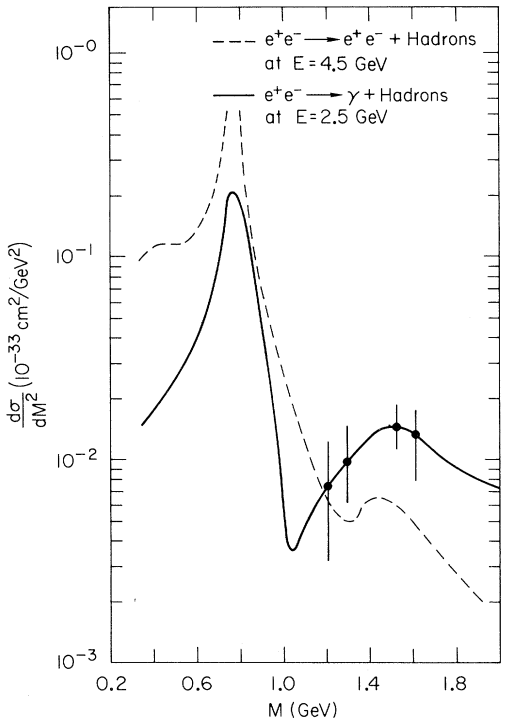

FIG. 6. Comparison of hadron production in inelastic electron Compton scattering and hard-photon bremsstrahlung; the error bars reflect the uncertainties of the measured e^+e^- cross sections.

$$\sigma_{\mu^+\mu^-}(M^2) = \frac{\pi\alpha^2}{M^2}\left(1 - \frac{4m_\mu^2}{M^2}\right)^{1/2} \times\left[1 + \frac{1}{3}\left(1 - \frac{4m_\mu^2}{M^2}\right) - \frac{4m_\mu^2}{M^2}\right], \tag{16}$$

where m_μ is the muon rest mass. Thus, for any other final state f, $\sigma_f(M^2)$ can be obtained from

$$\sigma_f(M^2) = \sigma_{\mu^+\mu^-}(M^2)\left(\frac{d\sigma^{e\gamma}}{dM^2}\right)_f \Big/ \left(\frac{d\sigma^{e\gamma}}{dM^2}\right)_{\mu^+\mu^-} \ , \tag{17}$$

A similar relationship is also valid for the bremsstrahlung process. In Figs. 3–5, we have plotted the cross sections for $\mu^+\mu^-$ production as given by Eqs. (6), (8), and (16). The background reactions of types (9) and (15) can be exactly calculated, and they are indeed very small. The detection of the $\mu^+\mu^-$ pair is similar to that discussed for the $\pi^+\pi^-$ pair.

IV. COMPTON PROCESS AS A BACKGROUND TO $\gamma\gamma^*$ ANNIHILATION

The reaction $e^- + \gamma \to e^-$ + hadrons is studied mainly to explore the hadronic structure of the real

photon in the same way as deep-inelastic electron-nucleon scattering is used to explore the structure of the nucleon. Since the differential cross section $d^2\sigma/d\nu\, dQ^2$, for $e^-\gamma$ scattering is estimated to be rather small, it is difficult to experimentally investigate the Q^2 and ν dependence of this cross section in detail. However, certain important features of the photon can still be learned by measuring the integrated cross section[7]

$$\sigma^{\gamma\gamma*}(\theta_{\max}, E) = \int_{Q^2 \geq Q_0^2;\ \nu \geq \nu_0;\ \theta \leq \theta_{\max}} \frac{d^2\sigma^{\gamma\gamma*}}{d\nu\, dQ^2}\, d\nu\, dQ^2 \tag{18}$$

and its moment[17]

$$\hat{\sigma}^{\gamma\gamma*}(\theta_{\max}, E) = \int_{\theta \leq \theta_{\max}} Q^4 \frac{d^2\sigma^{\gamma\gamma*}}{d\nu\, dQ^2}\, d\nu\, dQ^2 \tag{19}$$

as functions of $\theta_{\max}$ and E. The boundaries $Q^2 \leq Q_0^2$ and $\nu \leq \nu_0$ in Eq. (18) restrict the cross section to the deep-inelastic region, but these boundaries should not be essential for the "neutrinolike cross section" $\hat{\sigma}$, in the spirit of Bloom-Gilman duality. The contribution to the ee cross section relevant to the photon structure is obviously the two-photon process (1′), whereas the Compton process becomes the background in this case.[8] To get an estimate of the relative size between signal and background, we use a simple ρ-dominance model for the photon structure functions and assume $F_{1,2}^{\rho}$ to be similar in shape to the proton structure functions:

$$F_{1,2}^{\gamma}(x) \sim \frac{\alpha}{f_\rho^{\,2}/4\pi} F_{1,2}^{p}(x)\ . \tag{20}$$

Substituting Eqs. (7) and (20) into Eq. (18), we calculate $\sigma(\theta_{\max})$ for three different beam energies; the results are presented in Fig. 7. The contributions from the Compton process at these energies are plotted in the same figure for comparison. Since, at high beam energies, we have to integrate Eq. (6) over a region of $M \geq 5$ GeV where $\sigma_f(M^2)$ has not yet been measured, the Compton process contributions are approximated by $\sigma_f(M^2) = \sigma_f(25\ \text{GeV}^2) = 22$ nb and, for comparison, by $\sigma_f(M^2) = \sigma_f(25\ \text{GeV}^2) \times 25\ \text{GeV}^2/M^2$. As seen from the figure, the results are not sensitive to these two different assumptions since, over the kinematical range we have considered, the cross sections receive most of their contributions from $1 \leq M \leq 5$ GeV. The comparison of the moments $\hat{\sigma}^{\gamma\gamma*}$ as a function of the colliding-beam energy for these two processes is presented in Fig. 8 with a maximum electron scattering angle of 30°. Scaling models predict[17] $\hat{\sigma}^{\gamma\gamma*} \propto E^2$.

We want to point out a few significant features of our figures. As seen from Fig. 7, the even-C hadron production cross sections for $\gamma\gamma^*$ annihilation are almost saturated at small scattering angle[8] around 20° to 30°, since an increase of $\theta_{\max}$ corresponds to an increase of Q^2 and the $\gamma\gamma^*$ cross section is a rapidly decreasing function of Q^2. In parton models, this comes from the fact that, if the shape of the parton-antiparton distribution in the hadronic component of the photon is not too different from the parton distribution in the nucleon, the cross section $d\sigma^{\gamma\gamma*}/dQ^2$ behaves like $Q^{-4}\exp(-\text{const}\times Q^2)$ for Q^2 not too large. When the $\gamma\gamma^*$ cross sections start to become saturated, the Compton-process contribution to the odd-C hadron production cross section is still only a small fraction, about 1%, of the $\gamma\gamma^*$ cross section. Even if the moments are studied up to $\theta_{\max} = 30°$, we do not expect the background to exceed 20% of the signal. Thus, from a theoretical point of view, the Compton process does not lead to serious background problems for the measurements of the *partially integrated cross sections* and moments of inelastic electron-photon scattering. While only a very little increase for the $\gamma\gamma^*$ cross sections can be achieved by increasing $\theta_{\max}$ beyond 30°, the background, even though very

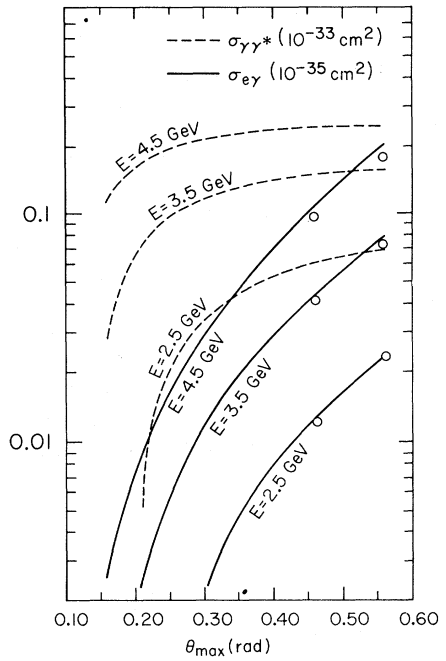

FIG. 7. Inclusive hadron production in real photon-virtual photon annihilation compared with the background from electron Compton scatterings; the cross sections represent events with $\nu \geq 1.5$ GeV^2, $Q^2 \geq 0.17$ GeV^2, and a maximum electron scattering angle $\theta_{\max}$; the little circles denote the size of the background if $\sigma(e^+e^- \rightarrow \text{hadrons})$ is supposed to fall off $\propto 1/s$ for $s > 25$ GeV^2.

small, increases rapidly with θ_{max}, since the larger the scattering angle, the closer the Compton amplitude approaches the u-channel pole. For large scattering angles, the $\gamma\gamma^*$ and Compton processes contribute comparable amounts to the increase in the integrated cross section, and hardly any additional information on $\gamma\gamma^*$ scattering can be obtained. This is related to the difficulty of studying the double-differential cross section $d^2\sigma^{\gamma\gamma^*}/dM^2 d\cos\theta$ at wide angles, as pointed out in Ref. 8. Thus, we conclude that measurements of the partially integrated cross sections of the type given by Eq. (18) and their moments are probably the most convenient way to study the structure of the photon.

V. DISCUSSION AND CONCLUSIONS

We have discussed equivalent secondary beams in high-energy positron (electron)-electron colliding beam machines and have studied cross sections for γe, e^+e^-, and $\gamma\gamma^*$ reactions. There are many other processes that can be considered. For example, as can be seen from the second term on the right-hand side of Fig. 1(a), the Compton process in the u channel can also be regarded as the annihilation of a secondary e^+ with the incident e^-, where the secondary e^+ is part of a virtual Bethe-Heitler pair (one real e^- and one almost on-shell virtual e^+), produced by the incident e^+. Obviously, the roles of the e^+ and e^- in the Bethe-Heitler pair can be interchanged. This interchange leads to the interesting situation that, at the cost of the size of the cross sections, e^+e^- processes can be explored with an e^-e^- colliding-beam machine and e^-e^- processes with an e^+e^- machine. The study of the former process is identical to our previous discussion of the Compton process, except that the background process (15) is no longer present. The study of the latter is something new, in particular in the high-energy region. However, even if the e^-e^- cross section is as large as the e^+e^- cross section for M being a few GeV [$\sigma_f(M^2)$ of the order of 20 nb], the resulting cross section for

$$e^+ + e^- \to e^+ + e^+ + e^{-*} + e^- ,$$

$$e^{-*} + e^- \to \text{anything}$$

might be too small for a feasible high-energy e^-e^- experiment performed with presently operating e^+e^- colliding-beam machines.

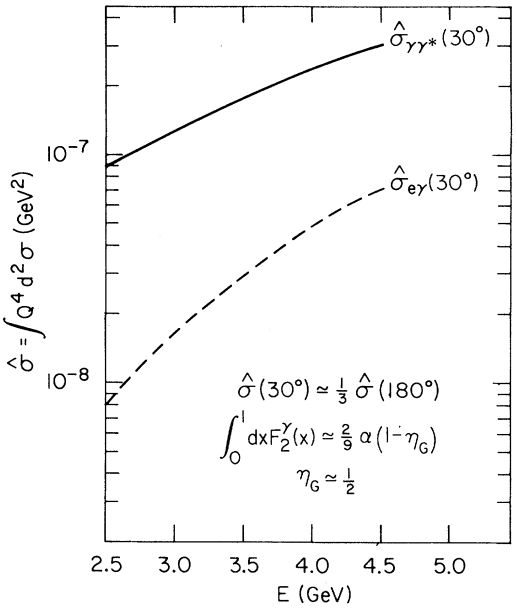

FIG. 8. Second moment in Q^2 of the cross section for inelastic electron-photon scattering for a maximum scattering angle of 30°; the solid line represents the two-photon mechanism while the broken line indicates the size of the Compton background. The estimates are based on a quark model with η_G denoting the fraction of the gluon momentum within the hadronic component of a photon in an infinite-momentum frame.

To conclude, we have studied Compton and bremsstrahlung processes in high-energy lepton-lepton collisions. At high beam energies and low values of M^2, the inelastic Compton process is most suitable for studying the behavior of the photon propagator, while at lower beam energies and moderate values of M^2, the bremsstrahlung process is favored. We also have discussed the role of the Compton process as a background to deep-inelastic electron-photon scattering. For the study of the photon structure, the Compton process is not a serious background as far as cross sections and moments for moderate electron-scattering angles are concerned.

ACKNOWLEDGMENTS

We gratefully acknowledge discussions with S. J. Brodsky and members of the SPEAR group. One of us (P.Z.) expresses his gratitude to S. D. Drell for the warm hospitality extended to him at SLAC.

*Work supported in part by the U. S. Atomic Energy Commission.

†Present address: Physics Department, University of Michigan, Ann Arbor, Michigan 48104.

‡Max Kade Fellow. On leave of absence from Technische Hochschule, Aachen, West Germany.

[1]C. F. von Weizsäcker, Z. Phys. 88, 612 (1934); E. J. Williams, Phys. Rev. 45, 729 (1934); F. Low, *ibid.* 120, 582 (1960); P. Kessler, Nuovo Cimento 17, 809 (1960); V. N. Baier, V. S. Fadin, and V. A. Khoze, Nucl. Phys. B65, 381 (1973).

[2]S. J. Brodsky, in *Proceedings of the 1971 International Symposium on Electron and Photon Interactions at High Energies,* edited by N. B. Mistry (Laboratory of Nuclear Studies, Cornell University, Ithaca, New York, 1971).

[3]In the last stage of our elaboration we received a report by N. Cabibbo and M. Rocca [CERN Report No. TH 1872-CERN (unpublished)] in which ρ production in inelastic electron Compton scattering was discussed.

[4]M. J. Creutz and M. B. Einhorn, Phys. Rev. Lett. 24, 341 (1970); Phys. Rev. D 1, 2537 (1970).

[5]D. Schildknecht, H. J. Willutzki, and G. Wolf, DESY Report No. DESY 71/28 (unpublished), and references quoted therein.

[6]T. F. Walsh and P. Zerwas, Phys. Lett. 44B, 195 (1973).

[7]In this context we are most interested in deep-inelastic electron-photon scattering, which has been worked out in detail by S. J. Brodsky, talk given at the Annual Meeting of the American Physical Society, New York, 1971 (unpublished); T. F. Walsh, Phys. Lett. 36B, 121 (1971); S. J. Brodsky, T. Kinoshita, and H. Terazawa, Phys. Rev. Lett. 27, 280 (1971); and C. E. Carlson and W.-K. Tung, Phys. Rev. D 4, 2873 (1971).

[8]J. Parisi, in Proceedings of the International Colloquium on Photon-Photon Collisions in Electron-Positron Storage Rings, Collège de France, Paris, 1973 [J. Phys. (Paris) Suppl. 35, C2-51 (1974)].

[9]V. Silvestrini, in *Proceedings of the XVI International Conference on High Energy Physics, Chicago-Batavia, Ill., 1972,* edited by J. D. Jackson and A. Roberts (NAL, Batavia, Ill., 1973), Vol. IV, p. 1.

[10]A. Litke *et al.*, Phys. Rev. Lett. 30, 1189 (1973); 30, 1349 (1973); B. Richter, talk given at the Conference on Lepton Induced Reactions, Irvine, 1973 (unpublished).

[11]In the examples we shall discuss, the photon energy will only be a small fraction of the incident positron energy.

[12]G. J. Gounaris and J. J. Sakurai, Phys. Rev. Lett. 21, 244 (1968).

[13]M. Gourdin, in *Hadronic Interactions of Electrons and Photons,* edited by J. Cumming and H. Osborn (Univ. of Glasgow, Glasgow, 1971).

[14]A. Zee, Phys. Rev. D 6, 900 (1972).

[15]S. D. Drell, Phys. Rev. D 7, 2190 (1973); I. Bars and M. B. Halpern, *ibid.* 7, 3043 (1973).

[16]M. S. Chanowitz, M.-S. Chen, and L.-F. Li, Phys. Rev. D 7, 3486 (1973).

[17]P. Zerwas, Phys. Rev. D 10, 1485 (1974).